Symmetry-mediated H_2O diffusion on Al{100}

Jibiao Li,* Ying Li, Shenglong Zhu, and Fuhui Wang*
State Key Laboratory for Corrosion and Protection, Institute of Metal Research (IMR), Chinese Academy of Sciences, 62 Wencui Road, Shenyang 110015, People's Republic of China

(Received 19 June 2006; revised manuscript received 26 July 2006; published 25 October 2006)

Based upon the full-electron *ab initio* calculations, we found orientational preferences and correlation for the atop-to-atop motions of an H_2O on Al{100}, which originates from the symmetry match between an H_2O and the surface square lattice. We have provided theoretical evidence that the favored mechanisms can be classical hopping coupled with either the molecular flipping or in-plane reorientations, with reduced energy barriers compared to those of the simple translational motions; while quantum tunneling assisted motion is not favored for an H_2O via the nearest neighbor diffusion.

DOI: 10.1103/PhysRevB.74.153415 PACS number(s): 68.43.Bc

Unlike site-to-site hopping of an adatom,[1] molecular surface motions (e.g., for H_2O) are not that straightforward due to their molecular symmetries, which create potential energy surfaces (PES) of high dimensions, even for a single H_2O molecule (C_{2v} symmetry) in surface diffusion.[2,3] This is referred to as the atop-to-atop motion. To understand water orientations in this elementary step, a consideration of the molecular degrees of freedoms is undoubtedly the key to a complete exploration of the PES, and therefore, is crucial to resolve the fundamental questions regarding coupling of molecular reorientations with lateral motion, orientation correlation, and roles of vibrational modes in surface motions. The last five years saw continuous efforts towards understanding water-metal interaction,[4] which is considered as a prototype model for initial wetting and corrosion. Various techniques, including quantum mechanical calculations[5] have been applied, wherein the consensus has been arrived at via adsorption geometries. Nevertheless, our current knowledge of molecular mechanisms of a single H_2O diffusion remains in its infancy.

In the present study, we have carried out all-electron *ab initio* calculations to map out a new picture of the nearest atop-to-atop diffusion for an H_2O on Al{100} and to shed new light on the molecular mechanisms of surface motions. We found that there exists an azimuthal correlation in the elementary step of the motion, and that the water monomer exhibits a concerted nature of molecular motion, with reduced energy barriers in contrast to that of the mechanism of simple lateral translation.

Our calculations have been performed using the density functional theory approach in Dmol code.[6] Electron exchange and correlation effects are described by the Perdew-Wang (PW91) generalized gradient approximation (GGA);[7] and the wave functions expanded in terms of the accurate double-numerical basis set with polarization functions (DNP). A Fermi smearing of 0.005 Hartree (Ha) was used to improve convergence efficiency. The clean Al{100} surface was modeled by a supercell of (3×3) size with a six-layer slab separated by a vacuum region of 12 Å. A single water monomer, without any constraints applied, was placed in unit cell to simulate the adsorption and surface diffusion. By placing an H_2O on the high symmetry sites (atop, bridge, and hollow), geometry optimizations were employed with the slab atoms fixed at the bulk truncated positions to identify minimum points of the PES. A Monkhorst-Pack mesh[8] with $3\times3\times1$ k-point sampling within the surface Brillouin zone was used. An optimization is considered converged when the energy per atom, mean displacement and mean force on the atoms are respectively less than 1×10^{-5} eV, 0.005 Å, and 0.05 eV/Å. Methods of linear synchronous transit (LST) and quadratic synchronous transit (QST),[9,10] were used to search for energy barriers of atop-to-atop diffusions $P(\omega_i,\omega_f)$ schematically shown in Fig. 1. The complete orientational combinations of the processes generate a set of diversified diffusion modes which involve water hopping motion combined with reorientations of either in-plane or out-plane rotation (flipping). The lateral translation with specific invariant azimuths proposed in Ref. 11 was examined for comparison purposes. The nudged elastic band (NEB) method,[12] has been used to map out the minimum energy paths (MEP) for the diffusions with the lowest energy barrier (0.17 eV), to ensure a thorough exploration of the PES has been performed.

Initial calculation of the lattice constant gave a value of 4.03 Å for bulk aluminum, in excellent agreement with the experiment value (4.05 Å). The structure of the isolated gas phase water for references was optimized within the same size of the supercell for water adsorption. The obtained structure shows that an H_2O has a bond length of 0.97 Å and a bond angle of 104.5°, which is in line with the experimental values of 0.96 Å and 104.5°, respectively. The monomer was found to adsorb preferentially on the atop site with a displacement of 0.13 Å from the precise on-top site. Two types of nonequivalent orientations ω^α and ω^β, were found as the most stable structures with the adsorption energy of −0.34 eV, where $\omega^\alpha=0,\pm\pi/2,\ \pi'$. $\omega^\beta=\pm\pi/4,\pm3\pi/4$ as defined in Fig. 1(a). These adsorption structures possess the maximum symmetry match between the H_2O (C_{2v}) and the substrate lattice. The obtained adsorption energy (−0.34 eV) and geometry are in good agreement with the previous result (−0.35 eV). Both H-up and H-down configurations over the bridge and hollow sites were found with the adsorption energy in the region of (−0.23,−0.18) eV. Thus, near atop sites (energy minima) serve as resting places for successive atop-to-atop motions. We also performed calculations for H_2O adsorption within different supercells of (2×2), (2×3), and (3×3) size (Table I), corresponding to coverages of 1/4, 1/6, and 1/9 ML, respectively. The coverage and cell-size effect was quite small, giving less than

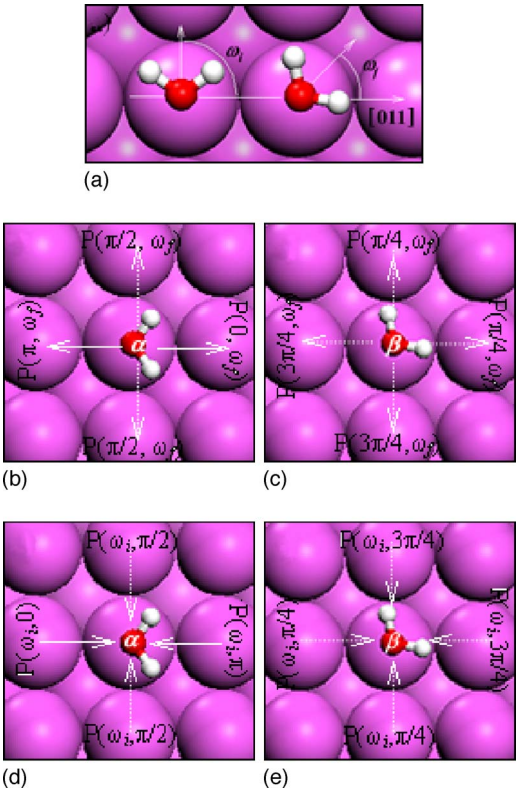

FIG. 1. (Color online) (a) Schematic diagram of the atop-to-atop motions for an H_2O on Al{100}. The two types of the obtained stable structures (α and β) were used as the initial and final states, and the corresponding azimuths (ω_i and ω_f) are defined as the angle between the twofold molecular axis and the atop-to-atop direction. The diffusion paths are denoted as the combinations $P(\omega_i, \omega_f)$, where ω_i, $\omega_f \in \{0, \pm\pi/2, \pi; \pm\pi/4, \pm 3\pi/4\}$. The investigated diffusion paths $P(\omega_i, \omega_f)$ are shown in (b) to (e), and the arrows stand for jump directions. The energy barriers $E(\omega_i, \omega_f)$ are listed in the Table II.

0.04 eV difference in adsorption energy of water on atop site. This suggests that the (3×3) super cell used here is large enough to avoid both water-water interactions and cell-size effect. Calculations with different numbers of slab layer (from 4 to 8) gave differences of adsorption energy within 5 meV, and the same conclusion has been obtained for water adsorption by employing different k points. These observations give us confidence in our following results of water diffusions.

TABLE I. Slab thickness (I), cell-size (II), and k-point (III) effect on adsorption energy of water monomer on near atop site. (3×3) unit cell was used for layer (I) and k-point (III) dependence.

I		II		III	
Layer	E (eV)	Cell (k-point)	E (eV)	k-point	E (eV)
4	−0.37	$2\times2(5\times4\times1)$	−0.30	$2\times2\times1$	−0.34
5	−0.36	$2\times3(4\times3\times1)$	−0.32	$3\times3\times1$	−0.34
6	−0.34	$3\times3(3\times3\times1)$	−0.34	$4\times4\times1$	−0.34
7	−0.35			$5\times5\times1$	−0.33
8	−0.35			$8\times8\times1$	−0.33

TABLE II. Energy barrier (E) distribution of atop-to-atop diffusions $P(\omega_i, \omega_f)$ for the specific initial and the final orientations. The second column shows the energy barrier range.

$P(\omega_i, \omega_f)$	$E(\omega_i, \omega_f)$ (eV)
$P(\pi, \omega_f)$ or $P(\omega_i, 0)$	0.17–0.22
$P(0, \omega_f)$ or $P(\omega_i, \pi)$	0.17–0.25
$P(\pm3\pi/4, \omega_f)$ or $P(\omega_i, \pm\pi/4)$	0.19–0.31
$P(\pm\pi/4, \omega_f)$ or $P(\omega_i, \pm3\pi/4)$	0.20–0.30
$P(\pm\pi/2, \omega_f)$ or $P(\omega_i, \pm\pi/2)$	0.21–0.38

In considering confined transitions, we obtained an energy barrier of only 33 meV for molecular flipping (e.g., $\alpha^0 \leftrightarrow \alpha^\pi$) and a much smaller value (only several meV) for molecular rocking (e.g., $\alpha^0 \leftrightarrow \alpha^{\pi/2}$). This suggests that both in-plane (rotational rocking) and out-plane (molecular flipping) reorientations are active due to the very small barriers, which in turn dominates the molecular behavior of the molecule within atop sites. These results further extend the previous DFT predictions that the molecular bending[13] or even the rotational motion,[14] with a relatively big angle, prevail at extremely low temperatures.

It is well accepted that the quantum tunneling probability of a particle is closely related to the shapes of energy profiles it experiences in a diffusion process. In our investigations, the potential energy curve $P(0, \pi)$ shown in Fig. 3 with extremely high curvature, motivated us to further ascertain if the water molecule adopts quantum tunneling as a way to move through the barrier over the bridge site. We solved numerically a one-dimensional (1D) Schrödinger equation with a quadric barrier of 0.25 eV and a barrier of 0.2 Å. However, the obtained molecular tunneling probability was zero in spite of the relative higher value (0.3) for a single hydrogen atom. This indicates that quantum tunneling assisted molecular flipping $P(0, \pi)$ is blocked for the atop-to-atop motion, bringing molecular mechanisms of surface motion into a classical regime.

A particularly interesting observation for the atop-to-atop motions shown in Table I, is that energy barriers of *alpha* (α) orientations initiated motions, irrespective of final orientations, diverge into two extreme energy distributions. A water molecule with the initial orientations (e.g., ω_i=0 or π) has obviously lowered barriers in the range (0.17–0.22 eV) which overlaps narrowly with (0.21–0.38 eV) of the initial orientations $\pm\pi/2$. This implies that an H_2O at atop site *does* have preferential orientations, with its twofold axis along the atop-to-atop direction, to initiate the motion [Fig. 1(b)]. This is also true for the orientations of the molecule when approaching the next nearest atop site [Fig. 1(d)].

To obtain a comprehensive view of the orientation dependence, we have constructed a contour map (Fig. 2) through numerical interpolation. For surface motion of an H_2O, which adopts low energy barriers whenever possible, this map further shows a strong azimuthal correlation between the initial (ω_i) and final angle (ω_f). The low barrier

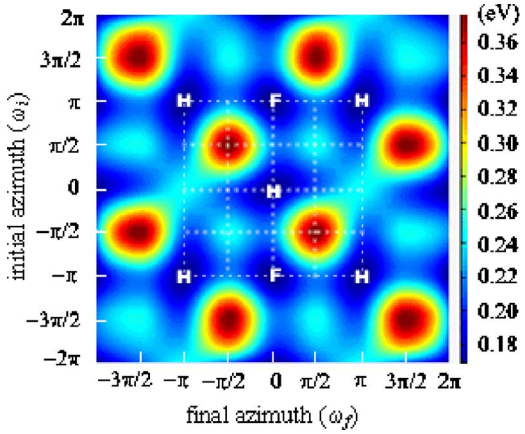

FIG. 2. (Color online) The contour map for activation energy $E(\omega_i,\omega_f)$ of atop-to-atop diffusions $P(\omega_i,\omega_f)$. $E(\omega_i,\omega_f)$ fluctuates periodically in the energy range of [0.17–0.38] eV. The minima (0.17 eV), $E(0,0)$, $E(\pi,\pi)$, and $E(\pi,0)$, are for diffusion modes of simple hopping (**H**) and flipping (**F**) respectively as shown in Fig. 3; while the maxima (0.38 eV) are located at $E(\pi/2,-\pi/2)$ and $E(-\pi/2,\pi/2)$. The dashed mesh is related to barriers of the diffusion paths shown in Figs. 1(b) to 1(e), and the azimuths are extended to 2π to get a whole view of each minimum.

(0.17–0.18 eV) regions around the minima (0.17 eV), represented approximately as $|\omega_i|+|\omega_f|<\pi/4$, $|\omega_i-\pi|+|\omega_f|<\pi/4$, and $|\omega_i|+|\omega_f-\pi|<\pi/4$, could account for this azimuthal correlation from an energetic perspective. Three azimuthal combinations $P(0,0)$, $P(\pi,0)$, and $P(\pi,\pi)$ have been identified as the most favored motions. Diffusion modes are symmetrically distributed over the map. Any combinations apart from the minima within those regions implies coupling of the molecular modes (e.g., molecular rotation or flipping) with lateral hopping. Therefore, molecular modes of water in real diffusion are closely related to the concerted nature of atop-to-atop diffusions as shown in Fig. 3(a). We also notice that all the extremum points (the maxima and minima) where orientation parameters corresponding to the simple equation: $|\omega_i-\omega_f|=0$ or $|\omega_i-\omega_f|=\pi$, where both ω_i and ω_f have the value of the *alpha* configuration (ω^α), thus implying that the most favored and unfavored motions are of the *alpha-to-alpha* case. This depends on the match degree of the molecular axis of both the initial and final orientation with the atop-to-atop direction, even though energy differences between various azimuthal orientations are negligible. An unexpected but interesting inference from the foregoing is that the molecular axis of symmetry serves as an indicator for a water monomer's intent of a nearest atop-to-atop motion. Such symmetrical pattern and correlation in which the energy barrier spans a wide range from 0.17 eV to 0.38 eV is in contrast with the homogenous pattern as well as observations from our study of water motion on Pd surfaces.[15] A significant insight from the results is that symmetry match controls not only water interactions with the surface,[16] but also molecular modes of the atop-to-atop motion.

In comparing the diffusion modes, we find that the obtained modes have low relative energies along the paths and therefore lowered barriers with respect to that of the lateral translation motion [Fig. 3(c)]. This suggests that lateral translation motion is weakly coupled to the surface and an H_2O in real motion neither retains the invariant orientation nor constant distance to the substrate lattice. Instead, dissipation of lateral translational energy proceeds by transferring energy into vertical displacements (hopping) and motions of orientation transitions whenever possible. For the flipping mode, the energy path is nearly degenerated with that of the molecular hopping, which indicates the strong coupling of out-plane rotation with lateral hopping. Additionally, we confirm that the relative energy of the equilibrium structure over the bridge site underestimates the energy barriers. This was also reported in Ref. 11, however, the reason for the discrepancy was not presented. We attribute this difference to excited energy paths which certainly exhibit higher energy barriers than the equilibrium energy of the optimized of ground state structure. For water motion in real case, the molecule is inevitably beyond the ground state.

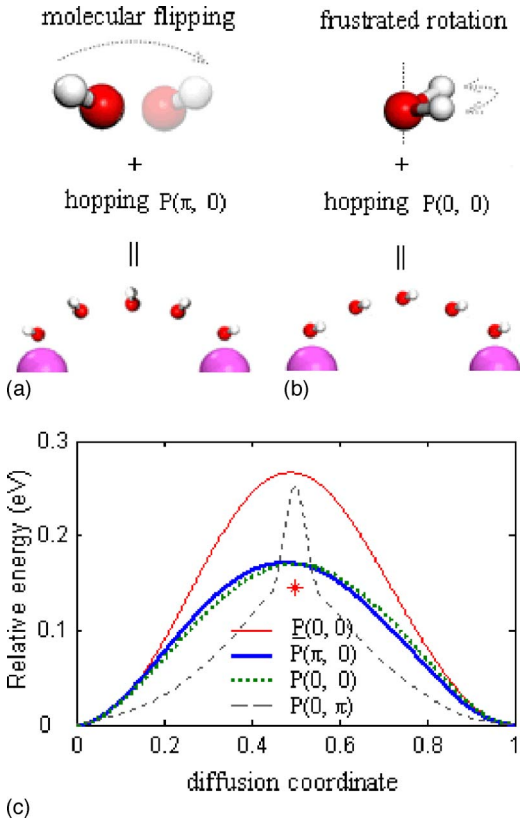

FIG. 3. (Color online) The candidate molecular mechanisms for the atop-to-atop motions of an H_2O on Al{100} (side view). (a) flipping mode for diffusion; (b) rotation mode for diffusion; the two modes are considered as the action of simple hopping concerted with molecule flipping or frustrated rotation; (c) NEB determined energy curves for the diffusion modes of simple hopping $P(0,0)$, molecular flipping $P(\pi,0)$, and $P(0,\pi)$. The energy profile for lateral translation $\underline{P}(0,0)$ is shown for comparison. The star (*) marks the relative equilibrium energy of the monomer over the bridge site, with respect to that of the stable structures at atop site.

From our results and analysis, we confirm that water hopping is one of the indispensable actions for the monomer in the atop-to-atop motions. Water orientations in the course of the diffusion are the key to uncovering the black box be-

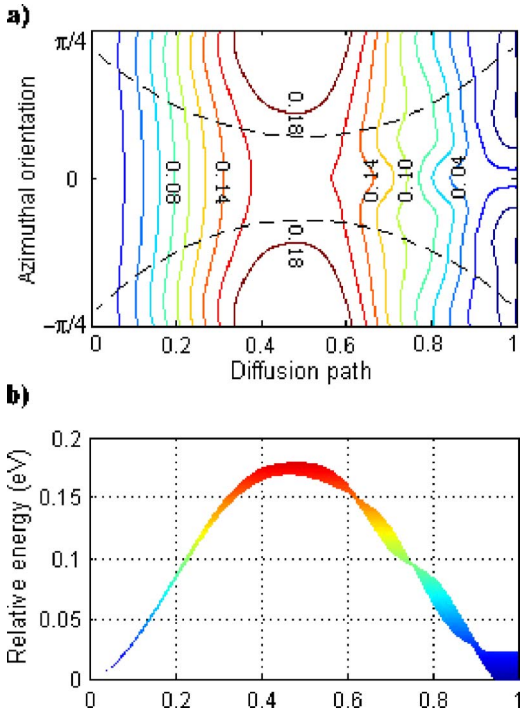

FIG. 4. (Color online) Azimuthal transitions in the course of the lateral hopping motion. a) The contour map of relative energy distribution as a function of azimuth and coordinate of the monomer in the atop-to-atop diffusions. Energy step of the contour lines has the value of 0.02 eV, and several energy values of the lines are shown. The map is constructed from series of path $P(\omega_i, \omega_f)$ within the lowest energy region $|\omega_i| + |\omega_f| < \pi/4$ in Fig. 2, where ω *varies from* $-\pi/4$ to $\pi/4$. (b) Projected energy surface of the selected region in map (a).

tween two nearest atop sites. It is interesting to consider how the concerted nature of motion is valid for couplings of other molecular modes (e.g., azimuthal reorientations) with the lateral hopping shown in Fig. 3(b). To detect such effect, we have built energy curves, as a function of the azimuth, into the contour map shown as Fig. 4(a). A striking characteristic of this map is that any diffusion paths within the region of dashed lines are found to have nearly degenerated relative energies [Fig. 4(b)] in the first half of the process. This necessitates the azimuthal transitions by which an H_2O transfers energy of fluctuation into active molecular reorientations with relative big angles, and therefore shows strong couplings of frustrated rotations with the lateral hopping. On the other hand, the corrugated surface with periodical feature of degenerated energy in the second half facilitates the coupling of molecular rocking with the lateral hopping, from energetic point of view. Such a picture is partially supported by the experimental investigation of inelastic electrons induced water motion on Pd(111) in which the energy of tunneling electrons is equivalent to that of the molecular bending mode.[17] Motivated by mode-selective chemistry,[18,19] which employs femtosecond laser pulse to change energy distribution within molecules on extremely short time scale,[20,21] we suppose that selectively control of the molecular modes of desired water diffusion (e.g., the identified flipping mode) can be achieved through electron-water interactions as well as photons or photon assisted electrons as a source to excite water monomers. This depends on how much energy is used to excite a specific vibration mode (e.g., O-H stretch or bending) of a water monomer confined within atop region. Ultrafast energy redistribution induced strong repulsive interaction of the oxygen atom with the surface makes molecular reorientation or flipping coupled lateral hopping feasible. We expect experimental efforts on observing these molecular mechanisms (flipping mode and rotation mode) for water diffusion on Al{100}.

In conclusions, we have shown that symmetry match between the monomer and the surface controls molecular modes of diffusions. There exists the azimuthal dependence and correlations for the classical over-barrier hopping diffusion, where an H_2O has preferential orientations in the elementary step of surface motion on Al{100}. Our results further predicts that the unique mechanisms of water hopping coupled with not only in-plane rotation but molecular flipping can be the molecular mechanism for an H_2O motion on Al{100}. Finally, the consideration of full molecular degrees of freedoms is of foremost importance in a molecular understanding of atop-to-atop motions, otherwise, diffusion barriers obtained would describe surface motion incorrectly, and a detailed diffusion mechanism involving molecular orientations will be hindered.

E. E. Oguzie and D. G. Lees are acknowledged for useful discussions.

*Author to whom correspondence should be addressed. Electronic address: jibiaoli@imr.ac.cn, fhwang@imr.ac.cn

[1] J. V. Barth, Surf. Sci. Rep. **40**, 75 (2000).
[2] T. Mitsui *et al.*, Science **297**, 1850 (2002).
[3] V. A. Ranea *et al.*, Phys. Rev. Lett. **92**, 136104 (2004).
[4] A. Verdaguer *et al.*, Chem. Rev. (Washington, D.C.) **106**, 1478 (2006).
[5] A. Michaelides, Appl. Phys. A (to be published).
[6] B. Delley, J. Chem. Phys. **92**, 508 (1990); *ibid.* **113**, 7756 (2000).
[7] J. P. Perdew *et al.*, Phys. Rev. B **46**, 6671 (1992).
[8] H. J. Monkhorst and J. D. Pack, Phys. Rev. B **13**, 5188 (1976).
[9] T. A. Halgren and W. N. Lipscomb, Chem. Phys. Lett. **49**, 225 (1977).
[10] N. Govind *et al.*, Comput. Mater. Sci. **28**, 250 (2003).
[11] A. Michaelides *et al.*, Phys. Rev. B **69**, 075409 (2004).
[12] G. Henkelman and H. Jonsson, J. Chem. Phys. **113**, 9978 (2000).
[13] S. Meng *et al.*, Phys. Rev. B **69**, 195404 (2004).
[14] S. Wang *et al.*, Phys. Rev. B **70**, 205410 (2004).
[15] J. Li *et al.*, Phys. Rev. B (unpublished).
[16] A. Michaelides *et al.*, Phys. Rev. Lett. **90**, 216102 (2004).
[17] E. Fomin *et al.*, Surf. Sci. **600**, 542 (2006).
[18] M. Citroni *et al.*, Science **295**, 2056 (2002).
[19] J. I. Pascual *et al.*, Nature (London) **423**, 525 (2003).
[20] L. Bartels *et al.*, Science **305**, 648 (2004).
[21] D. C. Jacobs, Nature (London) **423**, 488 (2003).